

A solar tracking system design based on linear switched reluctance motor

Norbert C. CHEUNG¹, Shi-Wei ZHAO¹, Wai-Chuen GAN²,
Zhen-Gang SUN¹, San-Chin KWOK¹

(1. Department of Electrical Engineering, Hong Kong Polytechnic University, Hong Kong Kowloon Hong Kong SAR, China;

2. ASM Assembly Automation Hong Kong Ltd., Kwai Chung Hong Kong SAR, China)

Abstract: A novel solar tracking scheme which adopts a linear switched reluctance motor(LSRM) as its servo actuator, is proposed in this paper. Three control schemes are designed for different requirements. The solar tracking system is divided into an electromagnetic subsystem and a mechanical subsystem, which are corresponding to the electromagnetic behaviors and the mechanical movement, respectively. The system controller has a cascaded structure, and two different controllers are designed for the two subsystems. Simulation results demonstrate the effectiveness of the modeling and the control scheme.

Key words: linear switched reluctance motor; solar tracking; sensorless control

一种基于直线开关磁阻电机的太阳跟踪系统设计

张 宙¹, 赵世伟¹, 简伟铨², 孙振刚¹, 郭新展¹

(1. 香港理工大学 电机工程系, 香港特别行政区 红磡;

2. ASM香港有限公司, 香港特别行政区 荃湾)

摘要: 本文提出了一个采用直线开关磁阻电机作为伺服机构的新颖的太阳跟踪系统. 同时也提出了三种控制器配置方案以满足不同需要. 按照电磁和机械特性, 该太阳跟踪系统可分解为一个电磁子系统和一个机械子系统. 整个系统的控制器采用级联控制结构, 分别对这两个子系统设计控制器. 仿真结果表明了其建模方法和控制器设计的有效性.

关键词: 直线开关磁阻电机; 太阳跟踪; 无传感器控制

中图分类号: TM615 文献标识码: A

1 Introduction

In renewable energy generation, photovoltaic(PV) systems play an important role since it acts as an alternative approach to employ solar energy and improve the system reliability with wind power generation. Owing to the rapid development of PV cells and the continuous drop of its price, the application of PV systems increases constantly in recent years. In order to obtain solar energy as much as possible, the study of the efficiency for PV systems has attracted many researchers' and engineers' attention. In general, there are three methods to increase the efficiency of PV systems^[1]. The first method is to increase the generation efficiency of solar cells; the second one is related to the energy con-

version system included maximum power point tracking(MPPT) control algorithms^[2,3]; and the third approach is to adopt solar tracking system to obtain maximum solar energy input from the sun^[4]. In a solar tracking system, DC motors are usually used to operate solar tracking system but it is expensive to maintain and repair.

A novel solar tracking scheme which adopts a linear switched reluctance motor(LSRM) as its servo actuator, is proposed in this paper. An LSRM has a simple and rugged structure; it is reliable and low in cost. Moreover, it is capable of operating in harsh environments. Three control schemes are designed for different requirements and will be discussed in the subsequent

sections.

2 System constructions and modeling

The proposed solar tracking system uses a three-phase LSRM as its actuator to drive the moving parts. The design schematic of the system is shown in Figure 1. A set of three-phase coils with the same dimensions is tightly fixed on the bottom of the motor. The three phase windings are separated 120 electrical degrees from one other. The moving platform is mounted on four wheels whose bearings are also supported on the bottom. Two linear guides are located between the moving platform and the wheels. This rugged mechanical structure can effectively buffer extended vibra-

tion during its operation. The stator track and the core of the windings are laminated with 0.5 mm silicon-steel plates, by means of which the motor manufacture can be simplified and the total cost is reduced greatly^[5]. A linear position sensor is integrated in the LSRM system to observe the motion profile and provides the feedback position information.

The PV cell arrays are linked to the gears which can be driven by the moving platform. The position of the sun is represented by using the angle A as shown in Fig.1. Also, the sun position can be translated to a displacement of the LSRM by multiple the A with its rotary radius L . Hence, the PV cell arrays can track the sun by properly operating the LSRM.

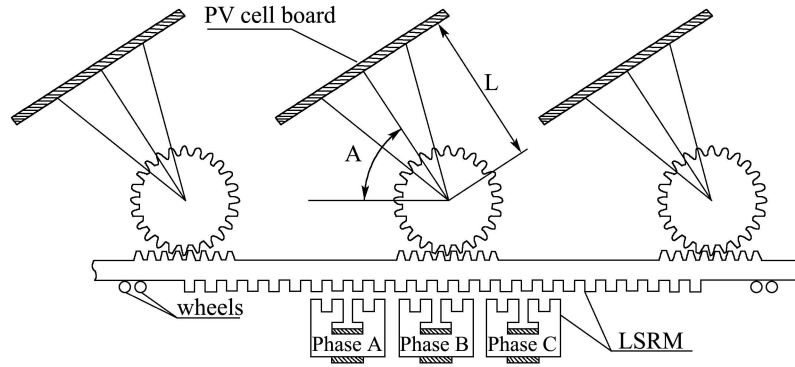


Fig. 1 The design schematic of linear switched reluctance-motor-based solar tracking system

The dynamic behavior of the whole system can be determined by Kirchhoff's Law on the voltage balance of individual phase coil, and by Newton's Law on the motor's mechanical motion. The equations of LSRM can be expressed as voltage equation(1) and mechanical equation(2). Since the flux linkage is a function of the current and position, the voltage equation can be further expressed as in equation(3), in which the second term on the right hand side corresponds to the voltage drop resulted by the current change and the third term corresponds to the one resulted by the position change.

$$V_j = r_j i_j + \frac{d\lambda_j}{dt}, \quad j = a, b, c, \quad (1)$$

$$f_e = M \frac{d^2x}{dt^2} + B \frac{dx}{dt}, \quad (2)$$

$$V_j = r_j i_j + \frac{\partial \lambda_j}{\partial x} \frac{dx}{dt} + \frac{\partial \lambda_j}{\partial i_j} \frac{di_j}{dt}, \quad j = a, b, c. \quad (3)$$

V_j is the applied voltage to phase j , i_j is the corresponding current, r_j is the resistance and λ_j is its flux linkage; f_e is the electromechanical force produced,

x is the displacement of the moving platform, M and B are the mass of the moving platform and the system friction constant respectively.

The connection between the two equations is the force producing function, by which the energy of the system is transferred from electromagnetic form to mechanical form. The total electromechanical force is the sum of the individual electromechanical force, as in equation(4). The force f_j produced by phase j is determined by differentiating the co-energy function with respect to position as equation(5)^[6]. The force produced is a nonlinear function of the position and phase current. Also, it can be seen that the force is a nonlinear function even though the magnetic circuit operates in its linear region, in which the phase force produced can be rewritten as equation(6). Here L_j is, named phase inductance, the ratio of the phase flux linkage by its current. The highly nonlinear characteristics of the driving system, therefore, are due to its nonlinear flux behavior and the mechanism of force

origination.

$$f_e = \sum_{j=a}^c f_j, \quad (4)$$

$$f_j = \frac{\partial}{\partial x} \int_0^{i_j} \lambda_j di_j, \quad (5)$$

$$f_j = \frac{1}{2} \frac{dL_j}{dx} i_j^2. \quad (6)$$

The response time of the electromagnetic behavior and mechanical motion are quite different. This is justified for our test setup since we can achieve the current loop bandwidth up to kHz while the output mechanical bandwidth is in the order of 10 Hz^[5]. Depending on the fact, the two-time-scale analysis is applied to model and design the driving system. The whole driving system is divided into two subsystems with different time scale named as fast and slow subsystem. In accord with the test results, the fast subsystem describes the electromagnetic behaviors of the coils while the slow subsystem corresponds to its mechanical motion. In this framework, the fast subsystem is considered by the treatment of the variables of slow subsystem as invariable. And it is also reasonable to describe the slow subsystem as the variables of the fast subsystem in their steady states. For a trajectory control system, the slow subsystem is a second-order differential equation(2) from the input of total force to the output of position. The fast subsystem is a first-order differential equation(3) for current control. Through this analysis, the complicated driving system can be divided into two tractable reduced-order subsystems and it is possible to design controllers to each subsystem respectively.

LSRM can be operated under open-loop mode as a stepper motor or close-loop mode as a servo motor. In servo mode, LSRM requires to be driven continuously. Hence, commutation is one of the essential tasks for a LSRM control for this operate mode. The desired force performance of a LSRM is always carried out by the synchronous commutation with its current position. Commutation, however, would bring problems of force ripples. To obtain smooth output force, a force sharing strategy can be applied.

For any given position, the phases of positive force produced and the phases of negative force produced can be represented by two sets as follows, $\Theta^+ = \{j : \frac{\partial L_j(x)}{\partial x} \geq 0\}$ and $\Theta^- = \{j : \frac{\partial L_j(x)}{\partial x} <$

$0\}$.

The force sharing strategy can be performed by a force distribution function (FDF):

$$\text{FDF}(x, f_d) = f_d \sum_{j=a}^c w_j, \begin{cases} f_d \geq 0, j \in \Theta^+, \\ f_d < 0, j \in \Theta^-, \end{cases}$$

where f_d is the desired total force and w_j is the weight of force for each phase. The selection of weight depends on the various force sharing strategies for different design purposes, but any force sharing strategy should satisfy that the sum of each weight should be 1.

3 Control strategies

According to the movement of the sun, the solar tracking system is a relative slow tracking application. On the other hand, the LSRM can be operated under different modes due to its construction characteristics. The controller of the solar tracking system, therefore, can take three schemes for different requirements as follows.

A) Open-loop scheme.

In this scheme, the LSRM is controlled under its open-loop mode as a stepper motor. This control scheme does not require linear position sensors for feedback and is simple to implement. The position precision of the control scheme is basically up to the step distance of the LSRM. Hence, this configuration scheme is suitable for low cost and common precision situations.

B) Servo scheme.

Also, the LSRM can be controlled under a close-loop mode as a servo motor. In servo scheme, a linear position sensor is required to provide feedback information. The control precision of this scheme usually can be rather high and depends on the sensor precision and control algorithm. Hence, the configuration scheme is suitable for high precision but high cost applications.

C) Sensorless scheme.

As a trade-off, the solar tracking system can be operated in a sensorless scheme. In this control scheme, the position information is estimated online and the controller adopts a close-loop format. This scheme can achieve relative high control precision over the open-loop scheme and the cost of the whole equipment can be lower than that of the servo scheme.

In this paper, the tracking system adopts a cascaded control structure. Two controllers are designed for the electromagnetic subsystem and mechanical subsystem corresponded to current control and position control, respectively. The two control subsystems are linked by the applied FDF. The block diagram of the whole driving system is shown as Fig.2. In the cascaded control system, the inner loop is for current control with fast variables and the outer loop is for the position control with slow variables.

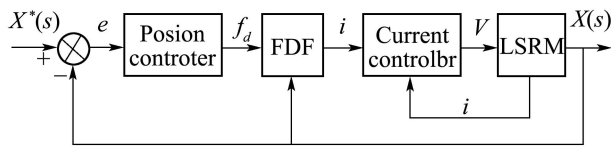


Fig. 2 Block diagram for the structure of whole control system

For each phase coil, the relation from terminal voltage to phase current can be represented as equation(7) by the rearrangement of equation(3). R_j is treated as a generalized resistor. The dynamic behavior of the electromagnetic subsystem, therefore, can be approximated as a first-order differential equation. As the inner loop, it can be easily regulated by a proportional controller to guarantee both stability and quick response.

$$L_j \frac{di_j}{dt} = V_j - R_j i_j, \quad R_j = r_j + \frac{dL_j}{dt}, \quad (7)$$

$$G(s) = \frac{1}{(Ms + B)s}. \quad (8)$$

Notice that if inner loop is to impose perfect current tracking, the mechanical motion can be equivalently represented as a second-order system (8). The gain from the input of desired force to the actual output force varies in a small region, the controller should be designed carefully to keep safe margin for the stability and dynamic performances of the whole driving system. For this system, a simple proportional-differential (PD) controller is sufficient for the position tracking as equation(9) and its closed loop transfer function is given by equation(10):

$$C(s) = K_p + K_d s, \quad (9)$$

$$\frac{X(s)}{X^*(s)} = \frac{K_p + K_d s}{Ms^2 + (K_d + B)s + K_p}, \quad (10)$$

where K_p and K_d are proportional gain and differ-

ential gain of the controller, respectively. Under the PD control, the system stability and high performance can be achieved by adjusting its controller parameters.

4 Simulation results

In this section, we illustrate the performance of the proposed models and control algorithm by simulation results. The simulations are performed with the MATLAB software package. The parameters of the LSRM system employed in the simulations are listed in the Table 1, and the applied FDF is chosen as in Table 2 [5].

Table 1 The main parameters of LSRM

Pole width	6 mm
Pole pitch	12 mm
Phase separation	10 mm
Winding length	30 mm
Wind width	25 mm
Air gap width	0.5 mm
Phase resistance	2.5 Ω
Aligned inductance	19.2 mH
Unaligned inductance	11.5 mH
Mass of the moving platform	5 kg
Friction constant	0.08 N \times s \times m ⁻¹

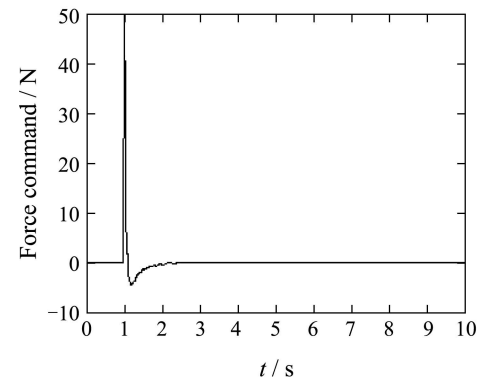
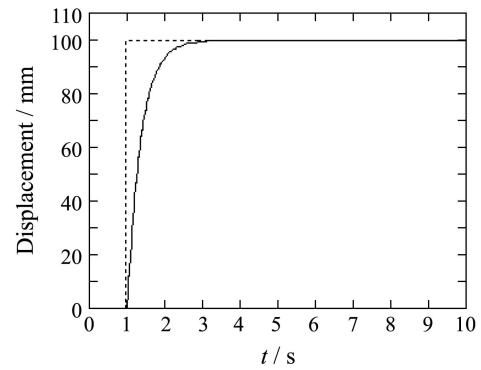


Fig. 3 Simulation: step response and control signal waveform

Figure 3 shows the simulation results on the response and control signal waveform by using the PD controller for a step tracking. It is clear that the system tracks the reference with good dynamical characteristics.

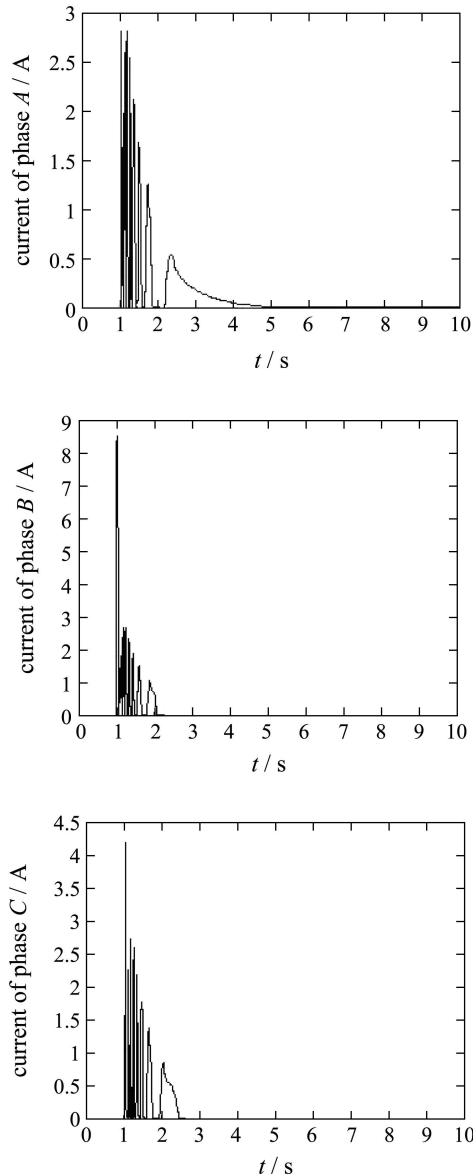


Fig. 4 Simulation: phase current waveforms for a step tracking

Figure 4 shows the three phase currents in the case of the step position tracking. Notice that all the phase currents are switched on and switched off continuously to perform the desired force. It is also seen that

the phase currents have quickly response and can be switched in a very short interval. This demonstrates the effectiveness of the modeling and controller design.

5 Conclusions

In this paper, a novel solar tracking system is proposed based on an LSRM. In addition, three control schemes are provided for different situations. The whole tracking system is modeled as two subsystems with different time characteristics. According to the applied system model, the system controller adopts a cascaded structure. The simulation results demonstrate that the system design is effective.

Table 2 Force distribution function (FDF) scheme

Position/mm	+ force command	− force command
0 ~ 2	$f_B = f_x$	$f_C = 0.5(2 - x)f_x$ $f_A = 0.5xf_x$
2 ~ 4	$f_B = 0.5(4 - x)f_x$ $f_C = 0.5(x - 2)f_x$	$f_A = f_x$
4 ~ 6	$f_C = f_x$	$f_A = 0.5(6 - x)f_x$ $f_B = 0.5(x - 4)f_x$
6 ~ 8	$f_C = 0.5(8 - x)f_x$ $f_A = 0.5(x - 6)f_x$	$f_B = f_x$
8 ~ 10	$f_A = f_x$	$f_B = 0.5(10 - x)f_x$
10 ~ 12	$f_A = 0.5(12 - x)f_x$ $f_B = 0.5(x - 10)f_x$	$f_C = f_x$

References:

- [1] PIAO Z G, PARK J M, KIM J H, CHO G B, BAEK H L. A study on the tracking photovoltaic system by program type[C]// *Proceedings of the Eighth International Conference on Electrical Machines and Systems*. Nan Jing, China: IEEE Press, 2005, 2: 971 – 973.
- [2] JAIN S, AGARWAL V. A new algorithm for rapid tracking of approximate maximum power point in photovoltaic systems[J]. *IEEE Power Electronics Letters*, 2004, 2(1): 16 – 19.
- [3] HO B M T, HENRY S H C. An integrated inverter with maximum power tracking for grid-connected PV systems[J]. *IEEE Transactions on Power Electronics*, 2005, 20(4): 953 – 962.
- [4] ARMSTRONG S, HURLEY W G. Investigating the Effectiveness of Maximum Power Point Tracking for a Solar System[C]// *Power Electronics Specialists Conference*. Recife, Brazil: IEEE Press, 2005: 204 – 209.
- [5] GAN W C, CHEUNG N C, QIU L. Position control of linear switched reluctance motors for high precision applications[J]. *IEEE Transactions on Industry Applications*, 2003, 39(5): 1350 – 1362.
- [6] MAJMUDAR H. *Electromechanical Energy Converters*[M]. Boston: Allyn and Bacon, Inc, 1965.